STRUCTURE, SCALE-SPACE AND DECAY OF OTSU'S THRESHOLD IN IMAGES FOR FOREGROUND/BACKGROUND DISCRIMINATION

R. Walia and R. Jarvis
Department of ECSE, Monash University, Clayton, Victoria-3028, Australia

Keywords: Scale-Space Theory, Pattern Recognition in Image Understanding, Segmentation and Grouping.

Abstract: A method for gauging the appropriate scale for foreground-background discrimination in Scale-Space theory is presented. Otsu's Threshold (OT) is a statistical parameter generated from the first two moments of a histogram of a signal / image. In the current work a set of OT is derived from histograms of derivatives of image having Scale-Space representation. This set of OT, when plotted against corresponding scale, generates a Threshold Graph (TG). The TG undergoes an exponential decay, in the absence of foreground and exhibits inflection(s) in the presence of foreground. It is demonstrated, using synthetic and natural images, that the maxima of inflection indicate the scale and threshold (OT) appropriate to interface edges. The edges identified by thresholding at scale and threshold given by inflection of OT correspond to foreground-background interface edges. The histogram inherently imbeds the TG with underlying image signal parameters like background intensity range, pattern frequency, foreground-background intensity gradient, foreground size etc, making the method adaptable and deployable for unsupervised machine vision applications. Commutative, separable and symmetric properties of the Scale-Space representation of an image and its derivatives are preserved and computationally efficient implementations are available.

1 INTRODUCTION

Scale-Space theory for image processing constitutes an important component of early vision (Lindberg, 1994). However, any pragmatic implementation of Scale-Space theory requires ascertaining the appropriate scale (Lindberg, 1994). This is a trivial task for well posed problems like in medical imaging where abundant apriori information (size, position, color, shape etc) is accessible. However, deciding the appropriate scale by machine vision is ill-posed for (a) images without access to apriori information e.g. in exploratory robotics wherein the environment changes continuously and unexpectedly, (b) evolutionary images like dynamic textures, anomaly detection in granite, wood, or in mining where apriori information is rendered redundant owing to evolution with each frame or image.

In addition to the problem of identifying the appropriate scale, there is often a requirement for identifying the foreground within an image. In this paper a novel method is proposed to identify both the appropriate scale as well as the foreground in the image at that scale by using the same parameter. The parameter used is Otsu Threshold (Otsu, 1979) for segmenting the image. This paper has following contributions:

(a) Surveys contemporary methods for scale identification and establishes the need to identify scale relevant to the whole image rather than local entities like pixels, edges, blobs etc.
(b) Proposes a novel method wherein scale is determined in response to global characteristics of image as opposed to local properties of images.
(c) Validates the method on a range of image parameters on synthetic and natural images and backgrounds.

2 SCALE IDENTIFICATION

Pioneering work by (Witkin, 1981), (Koenderink, 1984) and (Lindberg, 1994) has lead to Scale-Space

Walia R. and Jarvis R. (2009).
STRUCTURE, SCALE-SPACE AND DECAY OF OTSU'S THRESHOLD IN IMAGES FOR FOREGROUND/BACKGROUND DISCRIMINATION.
In *Proceedings of the Fourth International Conference on Computer Vision Theory and Applications*, pages 120-128
DOI: 10.5220/0001755101200128

theory. The basic tenant of this theory is to imbed a signal (image) into one-parameter of derived signals (images), the Scale-Space where the parameter denoted scale describes the image at the current level of scale. The image L(x,y) when expressed as a function of scale (t) is represented as L(x,y; t) and is obtained by convolving the image L(x,y) with a Gaussian kernel G(x,y;t) centered at point P(x,y) and having a variance t

$$L(x, y; t) = L(x, y) \otimes G(x, y; t) \tag{1}$$

where

$$G(x, y; t) = \frac{1}{2\pi t} e^{-\frac{x^2+y^2}{2t}} \tag{2}$$

2.1 Scale Identification Methods

(Lindberg, 1994) describes the problem of establishing an appropriate scale in the absence of apriori as intractable. Although models emulating mammalian vision take cognizance of the need to establish an appropriate scale they do not exclusively address this need, but rather skirt around it by using large scales (Malik. and Perorna, 1990) or contextual scales (Ren et al, 2006). (Lindberg, 1994) addresses scale identification in two different ways.

The first one involves a 4-Dimensional structure composed of a scale-space-blob generated from data driven structure detection in images. This structure is tracked over multi scales with the hypothesis that prominent structures persist across scales. Blobs are derived at different scales using monotonic gradients from local extrema and are then analyzed for their effective scale range using blob-descriptors like volume, contrast and area, and blob-events like annihilation, creation, merging and splitting.

In the second approach by Lindberg (Lindberg, 1994) utilizes the principle of non enhancement of extrema as applicable to Gaussian differential operators. A normalized (with scale) and consequently scale invariant Gaussian derivative operator is traced for maxima over scales. The scale corresponding to the maxima is heuristically hypothesized to coincide with the characteristic length of corresponding structure in image data. For a rigorous mathematical treatment, the reader is referred to chapter 13 of (Lindberg, 1994).

2.2 Drawbacks of Scale Identification Methods

These two methods are based on qualitative assumptions and mathematical derivations thereof. However these approaches have a “top-down” approach in tracing the entities (blob / edge of interest), wherein the entities are detected at a finer scale and their behavior traced to a coarser level. This approach has three drawbacks.

The first one arises from the use of local properties in the initial identification of entity which, in the case of blobs, is seeding originating from a blob event and, in the case of Gaussian derivative operator, is the edge maxima. Both these entities are dependent on local spatial properties like the intensity and nearness to another entity which often give rise to spurious structures. In the case of the Gaussian derivative operator, all the edges (including noise) are guaranteed a maximum (Lindberg, 1994) over some scale; hence the problem of appropriate scale identification still persists. To address this problem a ranking mechanism grades the entities based on properties of entities like contrast, life, spatial spread, volume etc across the scales. The ranking mechanism is unreliable as the local properties like the geometry of entity will influence both the Scale-Space evolution as well as the properties over scale. For example response to a Gaussian derivative of a curved edge will vary from that of a straight edge and, without apriori information on the kind of edge being detected, the response will be unreliable and in fact can often lead to a choice of improper derivative function.

The second drawback arises from the restricted spatial scope of local extrema. Fig 1 (a) shows a 1 dimensional signal (termed original) comprising of local maxima in the vicinity of global minima of the signal. The original signal is convolved with 3 Gaussian kernels as shown in Fig 1(b). The standard deviations of the 3 kernels coincide with the spatial spread of local extrema (Gauss 1), neighborhood of local extrema (Gauss 2) and the global neighborhood of local extrema (Gauss 3). The results of convolving with Gauss 1, Gauss 2 and Gauss 3 are also shown in Fig 1(a) by Result 1, Result 2 and Result 3, respectively. The evolution of local maxima is shown inside the dotted rectangle of 1(a). This evolution indicates that:

(a) Local extrema violates the principle of non-enhancement of extrema, as the intensity of local extrema is first reduced and then increased with increasing scale. This violation is not due to scale increment but due to consideration of local extrema in isolation from global neighborhood.

(b) Evolution of local maxima can have valid but conflicting classification depending on the scale. E.g. based on Result 1 the local extrema can be hypothesized as local maxima and based on Result 2 as global minima. There are two solutions to ascertain the appropriate classification. The first one (inapplicable in current context) is to have apriori information on the appropriate scale and the second is to have a global analysis rather than a local.

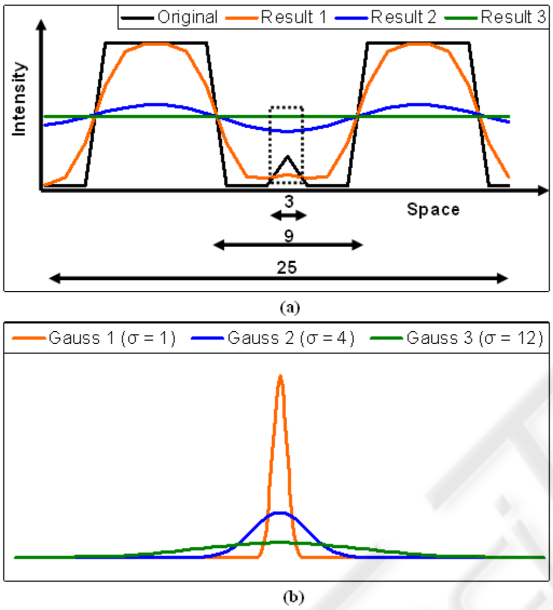

Figure 1: (a) 1D signal with spatial spreads of local extrema, local neighbourhood and global neighborhood and the results of convolution with Gaussian kernels at b. (b) Gaussian kernels corresponding to spatial spread of local extrema {Gauss 1, $\sigma = (3-1)/2$}, local neighbourhood {Gauss 2, $\sigma = (9-1)/2$}, global neighbourhood {Gauss 3, $\sigma = (25-1)/2$}.

The third drawback arises from a plausibly flawed hypothesis due to minimal representation of image. The methods (Lindberg, 1994) to identify appropriate scale omit the evolution of non-extrema neighborhood with scale. This neighborhood is quantitatively significant as locating even the first cut (zeroth scale) extrema involves discarding 8 neighboring pixels. Increasing the scale also increases the discarded neighborhood due to non-enhancement property. Hence the important structures are generated from a hypothesis based on a minimal representation of the image.

2.3 Proposed Method

In the current paper a "bottom-up" approach will be presented. In view of the drawbacks of establishing the optimum scale using local methods, the authors contend, that since incremental scales affect the extrema as well as the accompanying neighborhood, the impact of increasing Gaussian scales needs to be observed globally (entire image or a section of image that extends beyond the spatial extent of local feature) and not locally. To facilitate a global observation of the Scale-Space representation of entire image, it is desirable to have an image feature which can:

(a) Encompass the entire image.
(b) Embed underlying image signal features.
(c) Exist at all scales.
(d) Quantitatively identify the appropriate scale.
(e) Segregate important structures in the image.

Usage of Otsu's threshold as an image parameter for scale determination addresses the above requirements. Otsu's threshold is calculated at increasing scales from magnitude of Sobel edge of image, for identifying appropriate scale. Gray level Image Histograms derived from Scale-Space representation of images satisfies requirements (a) to (c). Otsu Threshold (Otsu, 1979) bifurcates an image thereby addressing requirement (e). Section 3 illustrates compliance with requirement (d) by creation of peaks when Otsu's Threshold is plotted against increasing scale. These peaks can be uniquely located and quantitatively defined.

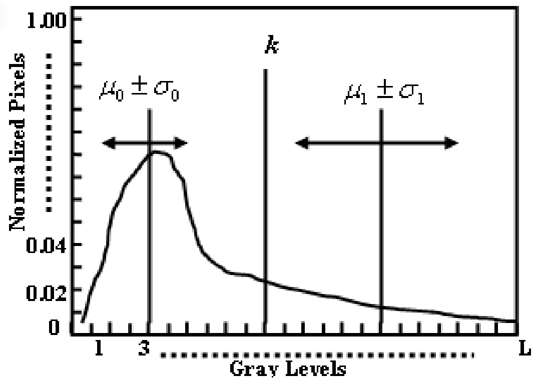

Figure 2: Visual representation of Otsu's Threshold.

Otsu's threshold (Otsu, 1979) is statistically generated from a normalized histogram for L gray levels in an image. Each gray level represents the pixels at that gray level as a percentage of total pixels in the image. This normalized histogram is bifurcated into two hypothetical classes C0 and C1 at a hypothetical threshold k. Hypothetical threshold (k), Mean and Standard Deviations of classes $C_0(\mu_0 \pm \sigma_0)$ and $C_1(\mu_1 \pm \sigma_1)$ are shown in Fig 2. The maximum of Between Class Variance (BCV) determines the appropriate threshold. BCV is defined as:

$$\nu_B = \omega_0(\mu_T - \mu_0)^2 + \omega_1(\mu_1 - \mu_T)^2 \tag{3}$$

Where

$$\omega_0 = \sum_{i=0}^{k} p_i \tag{4}$$

(0^{th} Order cumulative Moment for C_0)

$$\omega_1 = \sum_{i=k+1}^{L} p_i = 1 - \omega_0 \tag{5}$$

(0^{th} Order cumulative Moment for C_1)

$$\mu_T = \sum_{i=0}^{L} i p_i \tag{6}$$

(Mean Gray Level for the Image)

$$\mu_0 = \frac{\gamma_K}{\omega_0} \tag{7}$$

(Mean Gray Level for C_0)

$$\mu_1 = \frac{\mu_T - \gamma_K}{\omega_1} \tag{8}$$

(Mean Gray Level for C_1)

$$\gamma_K = \sum_{i=0}^{k} i p_i \tag{9}$$

(1^{st} Order cumulative Moment upto level k of histogram)

$$p_i = n_i / N$$

Normalised probability at level i ; (10)
n_i : number of pixels at level i;
N : Total pixels in image

While the Otsu's algorithm segregates the image, it does not classify foreground and background of segregated image in the absence of apriori information. Different segregation methods would be required for separating a darker foreground as compared to a brighter foreground for the same background. Usage of magnitude of Sobel edges in a image leads to uniformity of classification as the problem of distinguishing a foreground from background is transformed into one wherein interface (foreground-background) edges are required to be segregated from non-interface edges.

This method assumes that non-interface edges originate from homogenous textures (Foreground or Background) whereas interface edges arise from heterogeneous textures (Foreground and Background). It is therefore justifiably assumed that interface edges exhibit greater magnitude of gradient as compared to foreground-foreground or background-background edges, thus generating a group of edges amenable to segregation. Usage of first order derivative (sobel edges of an image) preserves the scale-space properties associated with zeroth order signal (original image) (Lindberg, 1994).

This approach addresses all the issues associated with scale identification listed in section 2.2 as the histograms are generated from magnitude of edges of entire image. The important structures are then segregated by bifurcation of the histograms. Since these structures originate from global calculations rather than local, they are relatively impervious to the local properties. The structures so obtained originate w.r.t. background and consequently do not require relative grading algorithms.

3 ALGORITHM & PROPERTIES: THRESHOLD GRAPH (TG)

Otsu's threshold is calculated for first derivative of the Gaussian smoothed image for each scale to generate a Gaussian Smoothed Derivative Image (GSDI). Specifically, magnitudes of Sobel's edges are used as a first derivative of Image. The algorithm for plotting the Threshold (Steps 1, 2), identifying the optimum scale (step 3) and identifying important structure in the GSDI (Step 5) is outlined in Algorithm 1.

Algorithm 1:

1. Convolve the image with Gaussian Kernel of increasing scale. For each scale :
   a. Calculate the histogram from Magnitude of Sobel edges.
   b. Calculate OT from the histogram.
   c. Record OT against the scale.
2. Plot OT against the scales.
3. Identify the scale at which local maxima exists in the TG. For all the results presented in this paper the local maxima was identified

by the maximum of difference operator (∇). Difference operator is defined as

$$\nabla_{2<=k<L}(k) = T(k) - T(k-1) \tag{11}$$

Where
L is the maximum scale under consideration
T (k) represents the Otsu's threshold at scale k
The optimum scale k^* is given by the maximum positive difference operator:

$$\nabla_{2<=k<L}(k^*) = \max[\nabla(k)] \tag{12}$$

If $\nabla(k) > 0$

4. Absence of any positive Difference Operator indicates absence of a foreground entity.
5. If an optimum scale with corresponding OT is identified, the image is segmented by Thresholding the GSDI with OT.

Note 1: Steps 3, 4 in algorithm 1 demonstrate that the process of detecting maxima and scale can be automated. The steps are not exhaustive and replaceable by other methods (beyond the scope of current paper) to detect maxima in signals.

3.1 Background Intensity Variation

The tiles in the Fig 3 are from images (Syn 1, 2, 3, 4, 5 and 6) of dimensions 640X480 with the intensities as listed in Table 1. The gradient magnitude between foreground and background of three sets of complimentary images (Syn 1, 4; 2, 5; 3, 6) is identical although the gradient direction of FG and BG is reverse. The TGs of complimentary sets of synthetic GSDIs are shown in Fig 4. Each complimentary pair has identical TG which leads to following two deductions:

(a) OT decay is exponential and proportional to the magnitude of gradient.
(b) Decay is independent of gradient direction.

Table 1: Intensities of Syn 1 to 6.

Image: (Syn)	1	2	3	4	5	6
Foreground Intensity	0	0	0	255	255	255
Background Intensity	85	170	255	170	85	0

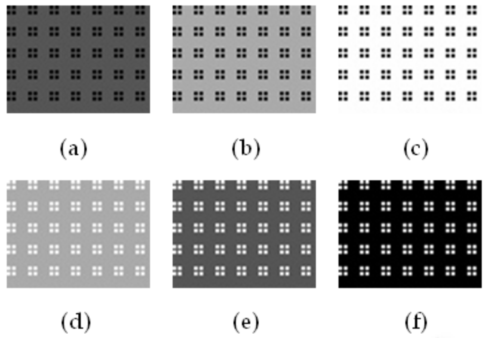

Figure 3: Tiles of Synthetic Images. (a) Syn 1 (b) Syn 2 (c) Syn 3 (d) Syn 4 (e) Syn 5 (f) Syn 6.

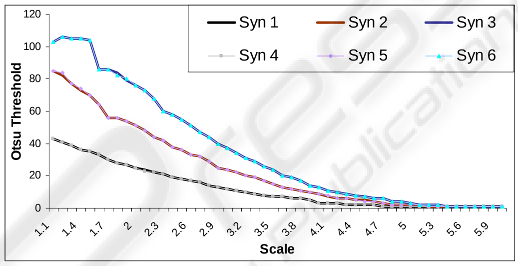

Figure 4: TG of Pairs Syn (1,4), (2,5), (3,6).

3.2 Background Intensity Variation

Tiles and TG from synthetic images Syn 10, 11, and 12 are shown in Fig 5. In each image pattern wherein the intensity is same but the frequency of background is varied. TG indicates that the OT decays with minor variations in decay rate due to background frequency.

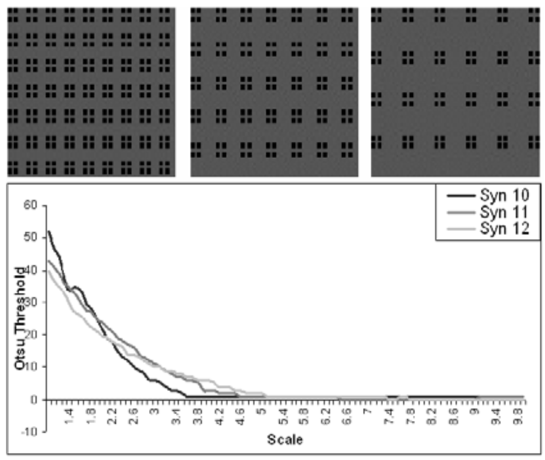

Figure 5: Top Row(Left to Right) – Tiles of Synthetic Images Syn 10,11 and 12. Bottom Row – TG of Syn 10,11 and 12.

3.3 Foreground Frequency Variation

In synthetic Images Syn 13, 14, 15 the background pattern comprises of square clusters of intensity 170 against a backdrop of intensity 85. The foreground comprises of cluster of four squares of intensity 255 and a size of 4 pixels each. These foreground clusters are separated by distance of 8, 16 and 24 for Syn 13, 14 and 15 respectively as illustrated by tiles in first column of Figure 6. The TG due to Algorithm 1 is shown in Figure 7.

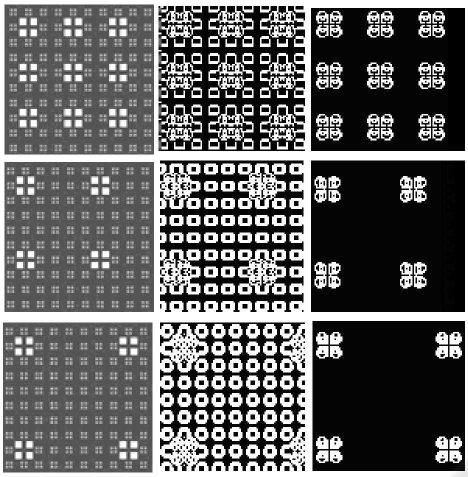

Figure 6: Top, Middle and Bottom Row: Images Syn 13, 14 and 15. First, Second and Third Column: Tiles of Synthetic Image, Thresholded Images at Lower Inflection point and Upper Inflection point.

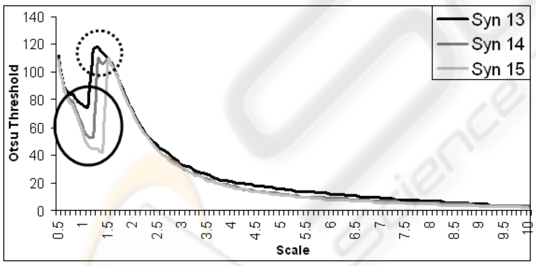

Figure 7: TG of Syn 13, 14 and 15.

The results of thresholding the image with the Otsu’s threshold at the lower and upper points of inflection are shown in second and third column of Fig 6. It is observed that the appropriate scale respect to the background of the image is given by the upper point of inflection. Column 3 of Fig 6 shows that the thresholded images at upper points of inflection give the important structure in the image with respect to the background. This quantitative event (maxima) enables TG to:

(a) *Detect scale and threshold appropriate to a image.*
(b) *Identify the important structures (in this case represented by edges) in the image.*

A slight shift in the local maxima is observed with decrease of the foreground frequency, which can be attributed to attrition in the percentage of pixels contributing to histogram bin at the background-foreground interface. Nevertheless the ability of the TG to adapt to the internal structure of the image background is illustrated.

3.4 Foreground Intensity Variation

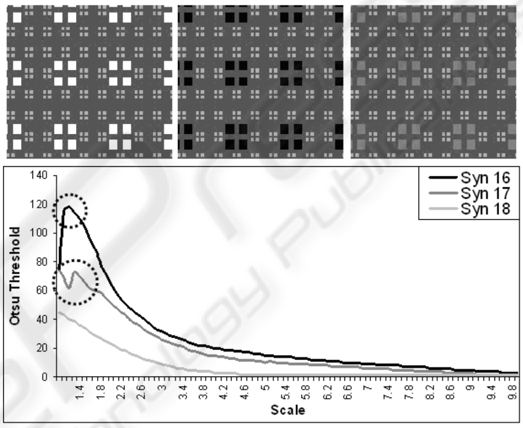

Figure 8: Top Row(Left to Right)- Tiles of Syn 16, 17 and 18. Bottom Row: TG of Syn 16, 17 and 18.

Images Syn 16, 17 and 18 shown in Fig 8 have the same pattern as the image Syn 13, however the foreground intensity is set to 255, 0 and 127 respectively. Since the background intensity varies between 85 and 170, three scenarios are:

i. Foreground intensity>Background range (Syn 16)
ii. Foreground intensity<Background range (Syn 17)
iii. Foreground intensity is within the Background range (Syn 18)

The TGs are depicted in Fig 8. Where the foreground intensity is beyond the background intensity range, inflection exists in the TG. However when the foreground intensity range is confined to the range exhibited by the background (TG for Syn 18) the inflection does not occur; hence the important structures are not detected. Absence of inflection can be attributed to similar interface derivatives as the non-interface derivatives. It is a unique case and does not occur frequently, especially in natural textures e.g. detecting a grass hopper in grass. Natural textures like pebbles, sand, water, hay, grass, vegetation, wood, and even manmade textures like rugs, carpets usually have background chromaticity which when projected onto gray scale has a narrow range. Consequently the foreground object's intensity exists outside the background image intensity range.

3.5 Foreground Size Variation

Three sets of synthetic images and their TG are shown in Fig 9 to 15 where Set 1 corresponds to Fig 9 (Syn 19 to 27) and Fig 12 (TG of Syn 19 to 27); Set 2 corresponds to Fig 10 (Syn 28 to 36) and Fig 13 (TG of Syn 28 to 36); Set 3 corresponds to Fig 11 (Syn 37 to 45) and Fig 14 (TG of Syn 37 to 45);. Each set of Synthetic images contains a rectangular foreground of varying sizes having area 0.01, 0.04, 0.09, 0.16, 0.25, 0.36, 0.49, 0.64 times that of the synthetic image. Reduced images are shown owing to paucity of space; however the background patterns are shown in top row second column of Fig 13, 15, 17 respectively for sets 1, 2 and 3. The thresholded GSDI at the points of inflection of TG for all the 3 sets are shown in:

(a) In 3 cases of background only i.e. Syn 19, 28 and 37 represented by black lines in Fig 14, 16 and 18 there is only decay of the TG without any inflection. Remaining TG of synthetic images however undergo an inflection even on introduction of foreground of area 1 % of total image area.

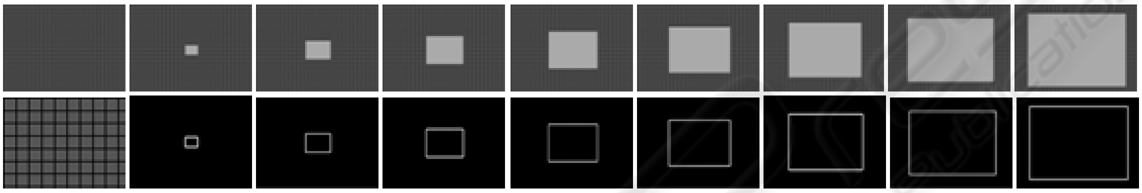

Figure 9: Top Row (Left to Right) Shrunk Images Syn 19 to 27. Bottom Row - Results. Bottom Row 1st Column: Background Pattern for Syn 19 to 27.

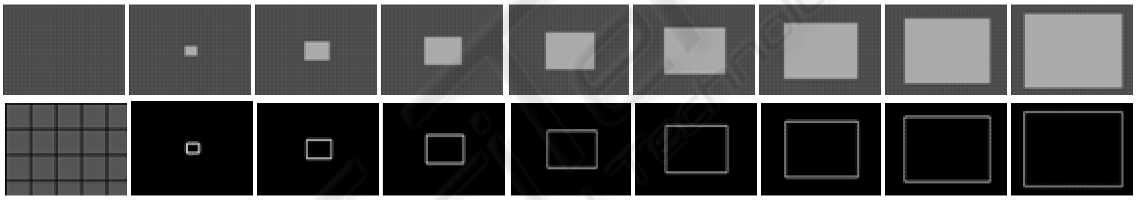

Figure 10: Top Row (Left to Right) Shrunk Images Syn 28 to 36. Bottom Row - Results. Bottom Row 1st Column: Background Pattern for Syn 28 to 36.

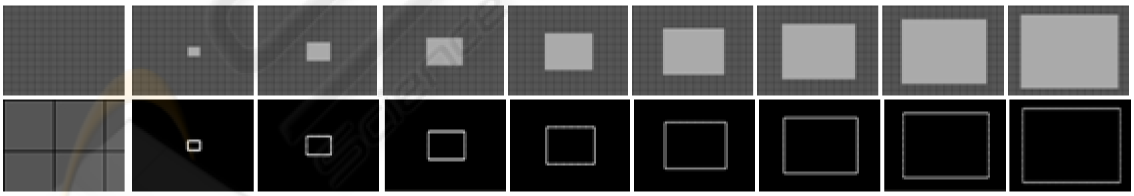

Figure 11: Top Row (Left to Right) Shrunk Images Syn 37 to 45. Bottom Row - Results. Bottom Row 1st Column: Background Pattern for Syn 37 to 45.

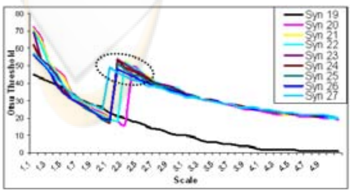

Figure 12: TG of Syn 19 to 27.

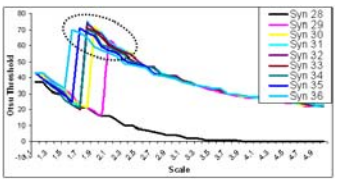

Figure 13: TG of Syn 28 to 36.

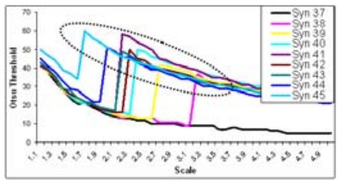

Figure 14: TG of Syn 37 to 45.

(b) Intra set points of inflection for all 3 sets reveal a decreasing trend (dotted ellipses) with increase of foreground area. The intra-set trend of decrease of non-interface class mean ($\Delta\mu_0$) being more than increase of interface class mean ($\Delta\mu_1$) results in decrease of threshold (k) due to equation 13 (Lin,2003)

$$k = (\mu_0 + \mu_1)/2 \qquad (13)$$

(c) Inter set points of inflection exhibit an increasing range of inflection values with respect to scale as shown by the dotted ellipses in Fig 12, 13 and 14. Background frequency is decreasing from set 1 to 2 to 3, hence threshold's (k) sensitivity increases to term (μ_1) in equation 13, resulting in increased range of inflection values.

3.6 Natural Images

Natural scenes comprise of a host of image signal distortion factors like ambient light, shadows, 2-D representation of 3-D space, occlusion and projection of 3-D chromaticity onto grayscale. There are image acquisition problems arising out of camera position, resolution and digital representation which aggravate the difficulty in estimation of appropriate scale. In addition a singular appropriate-scale as applicable to entire image will not exist in images wherein the coarseness of back ground pattern changes across the scene. In spite of inherent problems in locating the appropriate scale in natural images, OT is fairly robust in detecting background-foreground interface. Figures 15 to 18 present result of applying OT to various backgrounds both in the presence and absence of foreground.

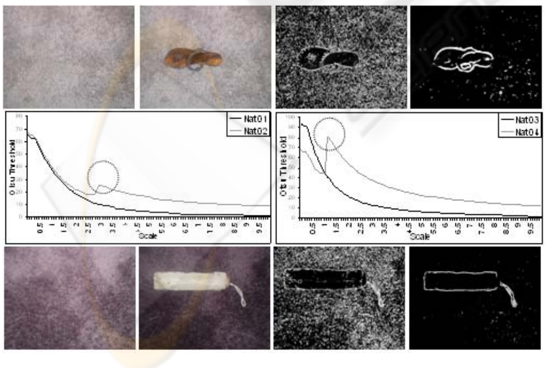

Figure 15: Top Row (Left to Right)-Natural Images Nat01 Nat 02, Thresholded Nat02 at lower and upper points of inflection. Middle Row-TG of Nat01, 02, 03 and 04. Bottom Row (Left to Right)-Natural Images Nat03 Nat04, Thresholded Nat04 at lower and upper points of inflection.

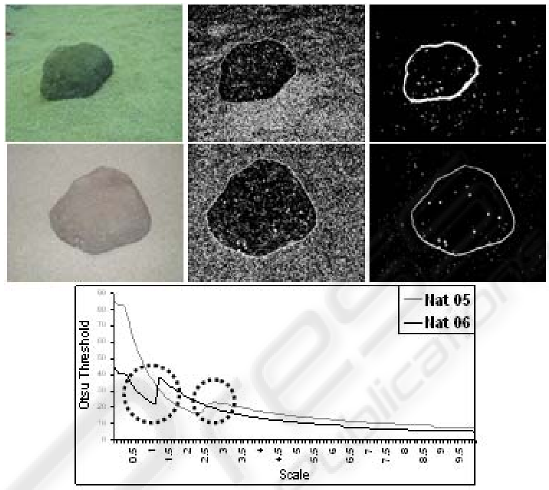

Figure 16: Top Row (Left to Right)-Natural Image Nat05 Original, and Thresholded at lower inflection point, and upper inflection point. Middle Row: Natural Image Nat06 Original, Thresholded at lower inflection point and upper inflection point. Bottom Row: TG of Nat05 and Nat06.

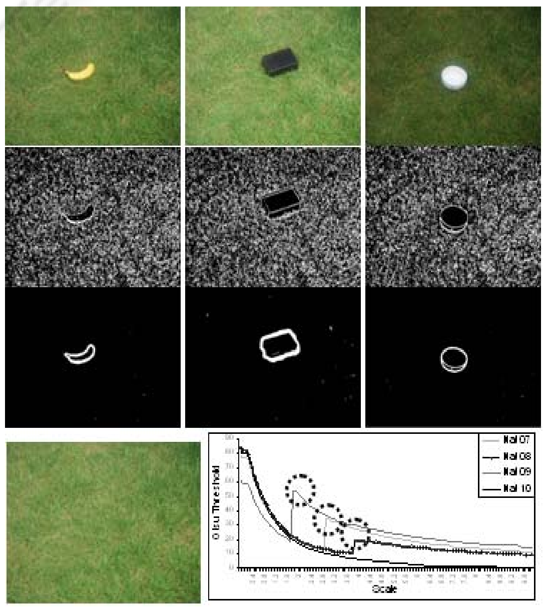

Figure 17: 1st Row (Left to Right)-Natural Image Nat07, Nat08, Nat09. 2nd Row: Nat07, Nat08 and Nat09 Thresholded at lower inflection points. 3rd Row: Nat07, Nat08 and Nat09 Thresholded at upper inflection points. Bottom Row: Nat10 and TG of Nat07, 08, 09 and 10.

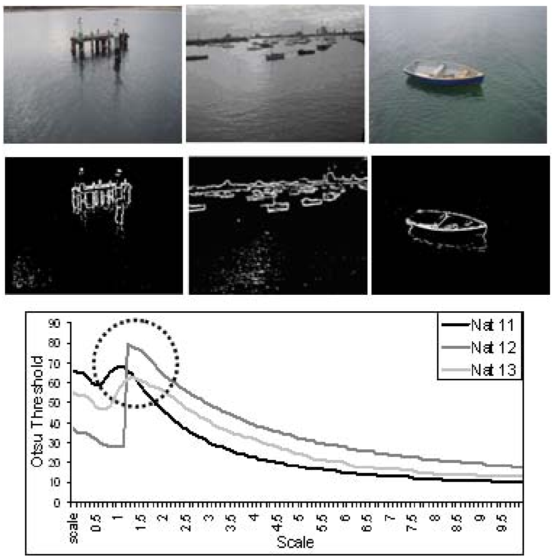

Figure 18: Row 1-Nat11, Nat12, Nat13, Row 4-TG of Nat11, 12, 13. Column 1 and 2 – Original and Thresholded Image (at upper point of inflection).

4 CONCLUSIONS

A novel “bottom-up” concept has been presented for identifying the important structures and appropriate scale using Scale-Space properties of images. The method is unsupervised and addresses the intractability of scale identification. Synthetic images have demonstrated the adaptability of the Threshold Graph to variations in the image. The results have also been demonstrated on natural and manmade textures.

This paper has dealt with the structures in reference to the whole image, but the same approach can be spatially reduced to find structures in regions of the images. Scale at points of inflection can also be used as a parameter in a variety of region based algorithms. Noise in results can be eliminated by one or combination of following

(a) Utilizing a scale higher than that of the inflection, as the important edges will persevere across scales.

(b) Hysteresis thresholding across scales.

(c) Sequentially thresholding the interface edges identified by Otsu’s threshold.

Future research would be on the pre-processing and post-processing required for extending the applicability of the TG. Another interesting application for which TG can be utilized is in establishing equivalence between space and time for dynamic textures exhibited by fluids, based on the assumption that the deformation of fluids in space and time is similar.

REFERENCES

Lindberg, T. *Scale Space Theory in Computer Vision*. Kluwer academic Publishers, Netherlands,. 1994.

Otsu. N. *A threshold selection method from gray-level histograms*. IEEE Transactions on Systems, Man and Cybernetics, SMC-9:62-66, Jan 1979.

Witkin A. *Scale-Space Filtering*. Proc. Int. Joint Conf on artificial Intel, Karlsruhe, Germany, 1019-1021, 1981.

Koenderink. J.J. *The Structure of Images*. Biological Cybernetics, vol 50, pp. 363-370,1984.

Malik. J. and Perorna. P. *Preattentive texture discrimination with early vision mechanisms.* J. Opt Soc Am A.,7(5): 923-32,1990.

Ren. X, Fowlkes. C and Malik. J. *Figure/Ground Assignment in Natural Images.* LNCS, Volume 3952-ECCV2006, pp 614-627, July 2006.

Lin. K.C. *Fast image thresholding by finding the zero(s) of the first derivative of between-class variance.* Machine Vision and Applications (2003) 13: pp 254-262.